Effects of Amphiphilic Topology on Self-Association in Solution, at the Air-Water Interface, and in the Solid State

D. Tyler McQuade, David G. Barrett, John M. Desper, Randy K. Hayashi, and Samuel H. Gellman*

Contribution from the Department of Chemistry, University of Wisconsin, Madison, Wisconsin 53706

Received July 25, 1994. Revised Manuscript Received March 10, 1995[⊗]

Abstract: The self-association of sodium carboxylates **1a**-**5a** in aqueous solution has been studied by ^{1}H NMR and dye solubilization. Amphiphile **1a**, the derivative of 1,6-methano[10]annulene bearing a carboxylate on the bridge carbon, is an example of a "contrafacial amphiphile", a rigid molecule with distinct polar and nonpolar faces. Amphiphiles **2a** and **3a**, the sodium salts of 2-naphthylacetic and 1-naphthylacetic acids, respectively, are isomers of **1a** with more conventional amphiphilic architectures. Amphiphiles **4a** and **5a** are derivatives of **1a** with extended nonpolar surfaces. Concentration-dependent ^{1}H NMR data indicate that self-association of **1a**-**5a** is weak and occurs in a stepwise fashion. Up to its aqueous solubility limit of 0.54 M, contrafacial amphiphile **1a** does not solubilize the hydrophobic dye orange OT, but conventional isomers **2a** and **3a** solubilize the dye above 0.33 and 0.50 M, respectively. Contrafacial amphiphile **4a** also does not solubilize orange OT, but **5a** does solubilize the dye. The properties of isomers **1a**-**3a** were compared also at the air-water interface, via tensiometry. Between zero and 0.15 M, naphthyl derivatives **2a** and **3a** cause a significant lowering of surface tension, but contrafacial amphiphile **1a** has little effect on surface tension up to 0.35 M. Crystal structures of carboxylic acids **1b**, **4b**, and **5b** show that the aromatic face of the 1,6-methano[10]annulene unit that is anti to the bridge engages in "herringbone" interactions with neighboring aromatic surfaces, which is similar to the behavior of conventional hydrocarbon aromatic moieties. The solid state packing patterns observed for **1b**-**3b** allow a speculative rationalization of the differences in surface activity among **1a**-**3a**.

Introduction

Amphiphiles, molecules that contain both hydrophilic and lipophilic moieties, play important roles in chemical and biological systems.[1] The most commonly studied amphiphilic architectures among small molecules involve relatively compact polar "headgroups" attached to long, flexible nonpolar "tails". Amphiphiles of this structural type readily partition to air-water interfaces, where they can maintain favorable headgroup hydration but avoid unfavorable tail hydration. In bulk aqueous solution, tail hydration is minimized by aggregation: amphiphiles containing a single tail (e.g., soaps and detergents) commonly form micelles, at low to moderate concentrations, and amphiphiles containing two tails (e.g., lipids) form bilayer structures. These variations in aggregate structure have been rationalized in terms of the relative sizes and shapes of the polar and nonpolar surface elements.[2]

Although amphiphiles with the polar headgroup/nonpolar tail topology have received the most attention,[1] the properties of a few amphiphiles with other types of architectures have also been examined. Such efforts have been focused largely on molecules that are available from natural (e.g., cholate[3]) or commercial sources (e.g., methylene blue[4]). Recently, however, there has been increasing interest in new synthetic amphiphiles with unusual architectures.[5-12] In some cases, the amphiphilic topology is related to naturally occurring examples, e.g., double-tail ammonium surfactants,[6] synthetic bolaamphiphiles,[7] and variously functionalized derivatives of cholate and related steroids.[8,9] In other cases, new topologies have been explored, e.g., the "molecular harpoons" of Regen et al.,[10] and "gemini surfactants".[11] Many synthetic systems display distinctive behavior. For example, the aggregation of ferrocene-containing surfactants is subject to redox control.[12]

We have been interested in species that we call "contrafacial amphiphiles", molecules that have rigid planar structures with one polar face and one nonpolar face (for our first discussion of the contrafacial amphiphile concept, see ref 13; Kahne et al. have noted the related topology of cholate and derivatives[9]). It seemed likely to us that contrafacial amphiphiles would have little or no tendency to self-associate in aqueous solution, or to

[⊗] Abstract published in *Advance ACS Abstracts*, April 15, 1995.

(1) For leading references, see: (a) Myers, D. *Surfactant Science and Technology*, 2nd ed.; VCH Publishers, Inc.: New York, 1992. (b) Fendler, J. H. *Membrane Mimetic Chemistry*; John Wiley & Sons: New York, 1982. (c) Lindman, B.; Wennerström, H. *Top. Curr. Chem.* **1980**, *87*, 1.

(2) (a) Mukerjee, P. *J. Pharm. Sci.* **1974**, *63*, 972. (b) Israelachvili, J. N.; Marcelja, S.; Horn, R. G. *Q. Rev. Biophys.* **1980**, *13*, 121.

(3) (a) Roda, A.; Hofmann, A. F.; Mysels, K. J. *J. Biol. Chem.* **1983**, *258*, 6362. (b) Mukerjee, P.; Moroi, Y.; Murata, M.; Yang, A. Y. S. *Hepatology* **1984**, *4*, 61S.

(4) Mukerjee, P.; Ghosh, A. K. *J. Am. Chem. Soc.* **1970**, *92*, 6403.

(5) See, for example: Nusselder, J.-J. H.; Engberts, J. B. F. N. *J. Am. Chem. Soc.* **1989**, *111*, 5000.

(6) Nakashima, N.; Asakuma, S.; Kunitake, T. *J. Am. Chem.* **1985**, *107*, 509.

(7) Fuhrhop, J.-H.; Fritsch, D. *Acc. Chem. Res.* **1986**, *19*, 130.

(8) Derivatives of cholic acid bearing modified polar groups on the flexible side chain have proven to be very useful for isolating and manipulating membrane proteins: Hjelmeland, L. M.; Nebert, D. W.; Osborne, J. C. *Anal. Biochem.* **1983**, *130*, 72.

(9) (a) Cheng, Y.; Ho, D. M.; Gottlieb, C. R.; Kahne, D.; Bruck, M. A. *J. Am. Chem. Soc.* **1992**, *114*, 7319. (b) Venkatesan, P.; Cheng, Y.; Kahne, D. *J. Am. Chem. Soc.* **1994**, *116*, 6955.

(10) Naka, K.; Sadownik, A.; Regen, S. L. *J. Am. Chem. Soc.* **1993**, *115*, 2278.

(11) (a) Parriera, H. C.; Lukenbach, E. R.; Lindemann, M. K. O. *J. Am. Oil Chem. Soc.* **1979**, *56*, 1015. (b) Menger, F. M.; Littau, C. A. *J. Am. Chem. Soc.* **1993**, *115*, 10083 and references therein.

(12) (a) Saji, T.; Hoshino, K.; Aoyagui, S. *J. Chem. Soc. Chem. Commun.* **1985**, 865. (b) Muñoz, S.; Gokel, G. W. *J. Am. Chem. Soc.* **1993**, *115*, 4899.

(13) Stein, T. M.; Gellman, S. H. *J. Am. Chem. Soc.* **1992**, *114*, 3943.

0002-7863/95/1517-4862$09.00/0

dwell at water–nonpolar interfaces, despite their display of considerable hydrophobic surface. This supposition (the "contrafacial amphiphile hypothesis") derives from topological considerations: contrafacial amphiphiles cannot aggregate to form topologically closed domains of their hydrophobic surface elements, with favorable nonpolar–nonpolar contacts in two or three dimensions, while maintaining polar group hydration. Traditional amphiphilic architectures, on the other hand, do allow such two- and three-domensional packing patterns, which is the origin of the distinctive properties of detergents, lipids, and related compounds. Molecules that display significant hydrophobic surface but do not self-associate or become localized at nonpolar–water interfaces might diffuse passively across biological membranes without disrupting the lipid bilayer's general impermeability toward polar species. If this anticipation were borne out, then contrafacial amphiphiles could aid drug delivery to intracellular targets.

Amphiphiles of low molecular weight with a facial segregation of polar functionality are uncommon. Here we describe a test of the contrafacial amphiphile hypothesis that employs the topologically distinctive 1,6-methano[10]annulene skeleton to achieve the required arrangement of polar and nonpolar surfaces.[14] Contrafacial amphiphile **1a** is compared to isomers

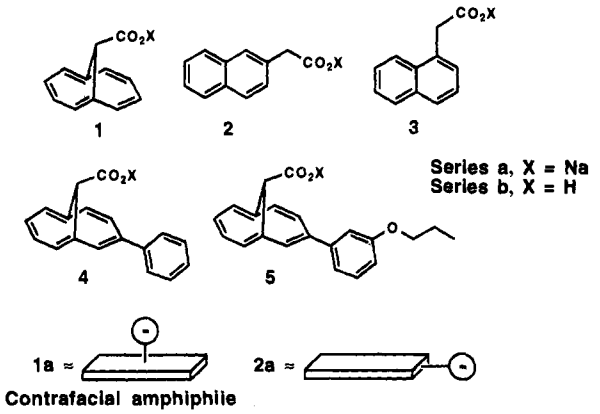

with more conventional amphiphilic topologies, **2a** and **3a**, at the air–water interface and in bulk aqueous solution. Although bridged annulene carboxylic acid **1b** was first prepared in the 1960s,[15] the relatively large quantities required for the studies reported below were not readily available until we devised an efficient new synthesis.[16] Our preparative route also gives access to unprecedented derivatives bearing substituents on the annulene ring that extend the nonpolar surface, e.g., **4b** and **5b**, and the properties of the corresponding carboxylates are described below.

Results

Surface Tension Studies. Figure 1 shows the effect of varying amphiphile concentration on the surface tension of an aqueous solution of **1a**, **2a**, or **3a**. For both naphthylacetates, a substantial decline in surface tension is observed as the carboxylate concentration is raised from 0 to 0.15 M. In contrast, contrafacial amphiphile **1a** causes relatively little diminution of surface tension up to 0.35 M. These observations suggest that the isomers of conventional topology, **2a** and **3a**,

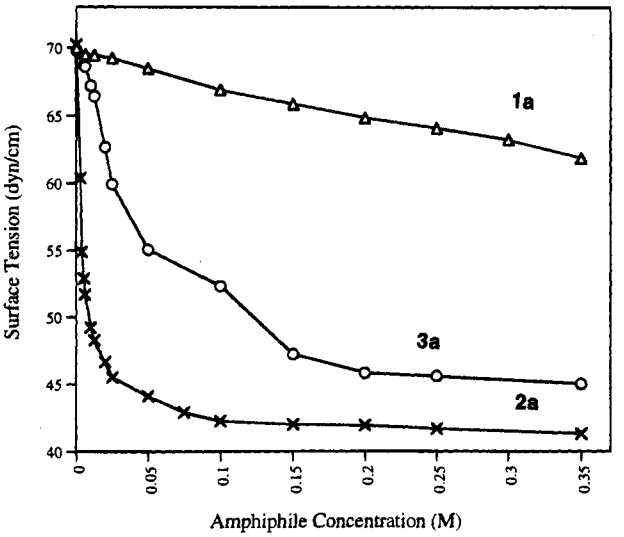

Figure 1. Surface tension of aqueous solutions of **1a** (Δ), **2a** (×), or **3a** (○) as a function of amphiphile concentration.

congregate at the air–water interface, but that contrafacial amphiphile **1a** has little tendency to reside at this interface. The limiting surface tension values for **2a** and **3a**, 41 and 45 dyn/cm, are close to the range of limiting values reported for the detergent sodium dodecyl sulfate (SDS), 48–52 dyn/cm.[17] For **1a**, on the other hand, the surface tension at 0.35 M is 62 dyn/cm.

Detection of Aggregation in Solution by Dye Solubilization. Solubilization of a hydrophobic dye is commonly used to detect aggregation of conventional amphiphiles,[18] and we have employed this method previously with amphiphiles of unusual architecture.[13] For micelle-forming amphiphiles, the concentration at which dye uptake begins is considered to be the CMC, and CMC values determined in this way are usually in agreement with values obtained from other techniques.[1] Presumably, the dye can be solubilized only when the amphiphiles create, via aggregation, a suitable nonpolar microenvironment in the aqueous medium.

Figure 2 shows results of orange OT solubilization experiments with isomers **1a**–**3a**. 2-Naphthylacetate **2a** begins to

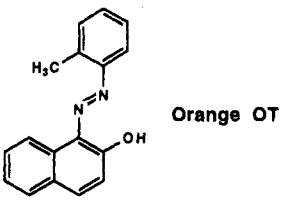

take up the dye at ca. 0.33 M, and isomer **3a** begins to take up the dye at ca. 0.50 M. In contrast, contrafacial amphiphile **1a** does not solubilize dye at any concentration up to the amphiphile's solubility limit of ca. 0.54 M. Figure 3 shows orange OT solubilization results for bridged annulene-based amphiphiles **4a** and **5a**; data for **1a** are also shown for comparison. Contrafacial amphiphile **4a** fails to take up dye at its solubility limit (ca. 0.16 M), but amphiphile **5a**, with a short flexible appendage, begins to solubilize orange OT at ca. 0.06 M.

Detection of Aggregation in Aqueous Solution by ^{1}H NMR. The onset of amphiphile self-association can often be detected by monitoring ^{1}H NMR chemical shifts as a function of concentration.[1] This approach is particularly useful when the amphiphiles contain π-systems, which lead to significant

(14) A preliminary account of these findings has been published: Barrett, D. G.; Gellman, S. H. *J. Am. Chem. Soc.* **1993**, *115*, 9343.
(15) Vogel, E. *Spec. Publ.-Chem. Soc.* **1967**, *No. 21*, 113.
(16) (a) Barrett, D. G.; Liang, G.-B.; Gellman, S. H. *J. Am. Chem. Soc.* **1992**, *114*, 6915. (b) Barrett, D. G.; Liang, G.-B.; McQuade, T. M.; Desper, J. M.; Schladetzky, K. D.; Gellman, S. H. *J. Am. Chem. Soc.* **1994**, *116*, 10525.
(17) Mysels, K. J. *Langmuir* **1986**, *2*, 423.
(18) Schott, H. *J. Phys. Chem.* **1966**, *70*, 2966.

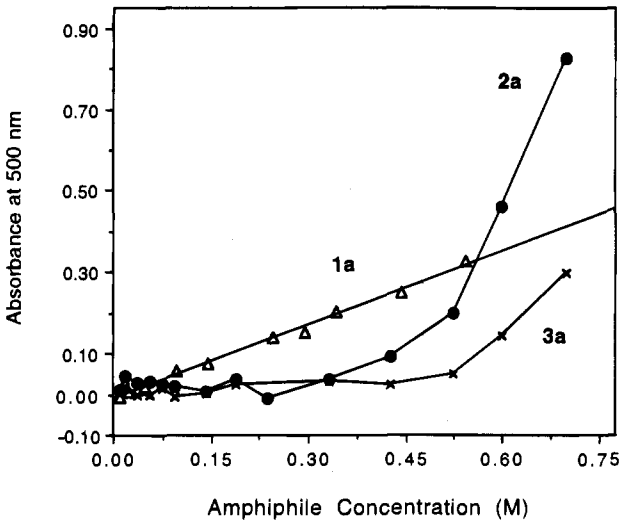

Figure 2. Orange OT solubilization by aqueous solutions of **1a** (Δ), **2a** (○), or **3a** (×), as a function of amphiphile concentration. The line for **1a** is the result of linear regression, and the lines for **2a** and **3a** are arbitrary. The experimental protocol is described in the Experimental Section. The electronic absorption of bridged annulene **1a** (but not naphthalene derivatives **2a** or **3a**) "tails" weakly out ot 500 nm, which causes the small amount of absorbance seen for concentrated solutions of **1a**.

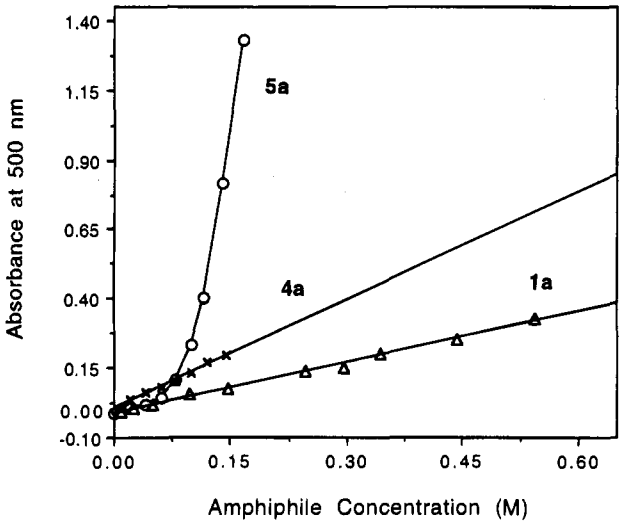

Figure 3. Orange OT solubilization by aqueous solutions of **1a** (Δ), **4a** (×), or **5a** (○), as a function of amphiphile concentration. The lines for **1a** and **4a** are the results of linear regression, and the line for **5a** is arbitrary. The experimental protocol is described in the Experimental Section. The electronic absorption of the bridged annulenes "tails" weakly out to 500 nm, which causes the small amount of absorbance seen for concentrated solutions of **1a** and **4a**.

chemical shift dispersion between aggregated and nonaggregated states, and when an individual amphiphile's exchange between aggregated and nonaggregated states is rapid on the NMR time scale. (This latter condition holds for spherical micelles and for less cooperatively formed aggregates, but not for bilayer vesicles.) We have recently demonstrated quantitative agreement between the information on self-association obtained from variable concentration NMR data and the information obtained from orange OT solubilization data for synthetic amphiphiles containing an ethanoanthracene-based headgroup.[13]

Figure 4 shows the concentration dependence of one ^{1}H NMR resonance for **1a** and one resonance each for isomers **2a** and **3a**. Amphiphiles **1a**–**3a** display concentration-independent chemical shifts below 0.02–0.04 M. Above these concentrations, the upfield shifts of the resonances monitored are a gradual function of concentration, up to each carboxylate's solubility limit. The upfield shifts suggest that **1a**–**3a** begin to self-associate at relatively low concentrations in aqueous solution, but these data do not provide conclusive evidence of aggregation because the range of chemical shift variation is small in each case (<0.1 ppm). Since the chemical shifts vary gradually, any aggregation that occurs must be non-cooperative (i.e., the self-association does not correspond to classical micelle formation). Identical conclusions were drawn from the concentration-dependent behavior of other proton resonances from **1a**, **2a**, and **3a**.[19]

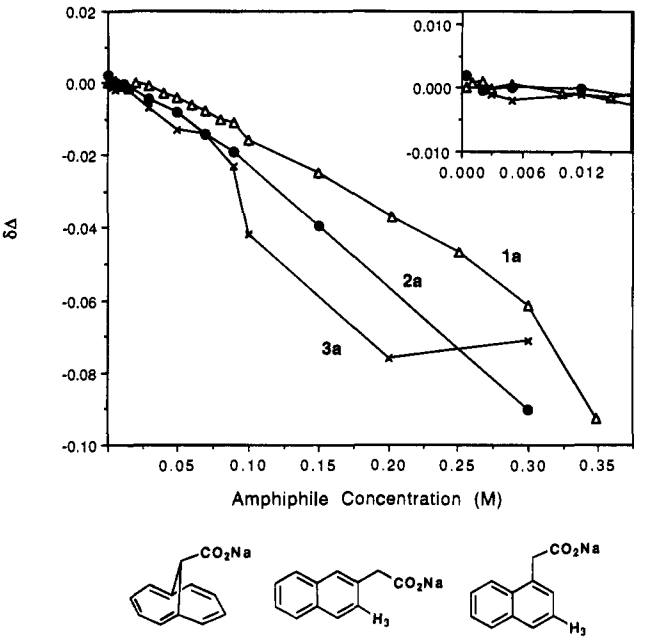

Figure 4. Concentration dependences of ^{1}H NMR chemical shifts: **1a**, monitoring the center of the BB′ component of the aromatic AA′BB′ pattern (Δ); **2a**, monitoring H_3 (○); **3a**, monitoring H_3 (×). In each case, the data are analyzed as relative chemical shifts, referenced to the actual chemical shift at the lowest concentration examined. The lines are arbitrary.

Figure 5 shows the concentration dependence of one ^{1}H NMR resonance for **4a** and one resonance for **5a** (data for **1a** are shown for comparison). Both **4a** and **5a** display concentration-independence below ca. 0.005 M, and both display gradual upfield shifts above the onset concentration, up to 0.15 M, which is near each amphiphile's solubility limit. For contrafacial amphiphile **4a**, the total range of chemical shift variation is small (ca. 0.1 ppm); therefore, this variation is merely suggestive of aggregation. For **5a**, the range of variation is nearly 0.5 ppm, which is strong evidence for self-association. In both cases, the gradual nature of the concentration-dependent changes indicates that any underlying aggregation is non-cooperative. The concentration-dependences of other resonances from **4a** and **5a** led to similar conclusions.[19]

Figure 6 shows the concentration dependence of one ^{1}H NMR resonance for **6**. In contrast to **1a**–**5a**, **6** shows a substantial change in chemical shift over a relatively narrow concentration range (note the differences in horizontal scale among Figures 4–6). Further, there is a sigmoidal relationship between chemical shift and concentration range, with regions of relative insensitivity at concentrations higher and lower than the range of high sensitivity. This behavior indicates that **6** aggregates

(19) Barrett, D. G. *Ph.*D. Thesis, University of Wisconsin–Madison, 1993.

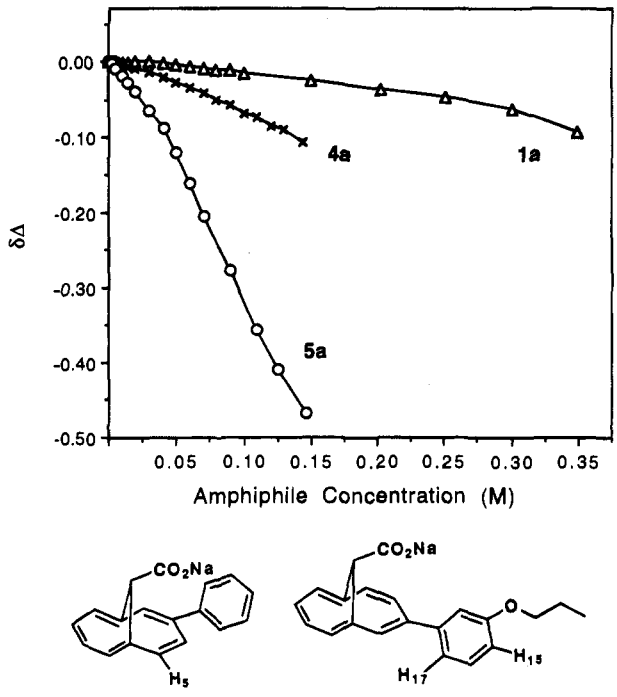

Figure 5. Concentration dependence of ^{1}H NMR chemical shifts: **1a**, monitoring the center of the BB′ component of the aromatic AA′BB′ pattern (Δ); **4a**, monitoring H_5 (×); **5a**, monitoring a resonance arising from either H_{15} or H_{17} (○). In each case, the data are analyzed as relative chemical shifts, referenced to the actual chemical shift at the lowest concentration examined. The lines are arbitrary.

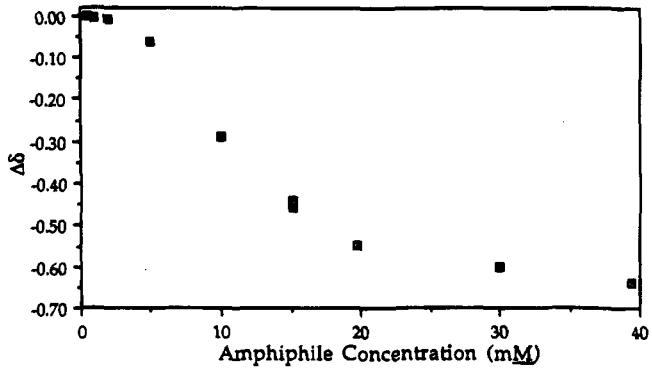

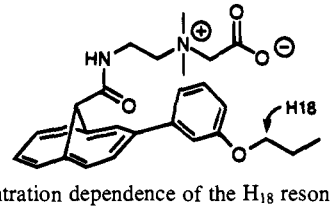

Figure 6. Concentration dependence of the H_{18} resonance of **6**. The data are analyzed as relative chemical shifts, referenced to the actual chemical shift at the lowest concentration examined.

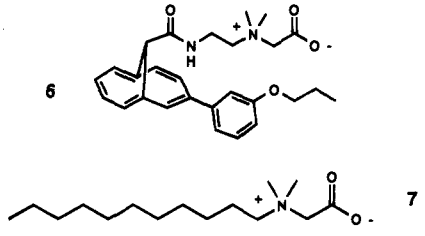

more cooperatively than do **1a**−**5a**. In order to determine a CMC, one typically recasts data like those in Figure 6 as a plot of chemical shift vs inverse amphiphile concentration.[1,20] Figure 7 shows such a plot, along with the lines resulting from linear

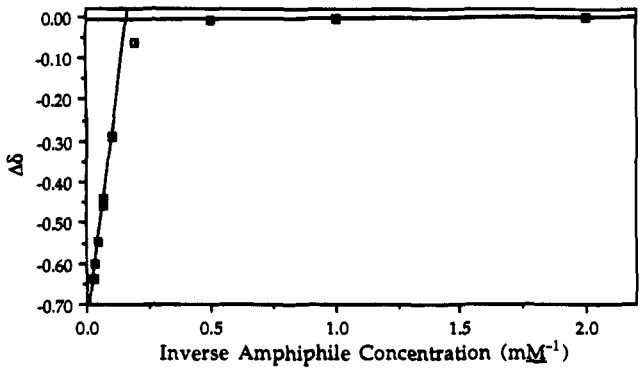

Figure 7. Plot of $\Delta\delta$ (H_{18}) of **6** (defined relative to the absolute chemical shift at the lowest concentration) as a function of the inverse of the concentration. The two lines shown are derived from linear regression of the data points for the three highest and the three lowest concentrations. The intersection of these lines occurs at 0.17 mM^{-1}.

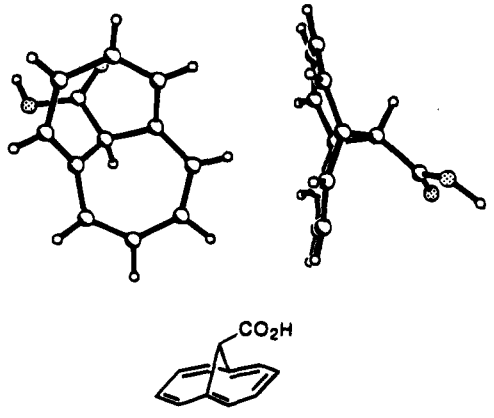

Figure 8. Ball-and-stick representation of a neighboring pair of molecules in the crystal lattice of **1b**; the angle between the mean planes of the annulene rings is 67°.

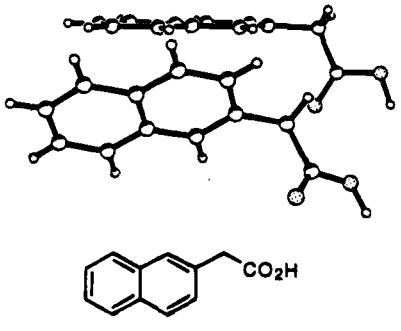

Figure 9. Ball-and-stick representation of a neighboring pair of molecules in the crystal lattice of **2b**; the angle between the mean planes of the naphthyl groups is 48°.

regression analysis of data points from the three lowest concentrations and the three highest concentrations. The intersection of such lines is taken to define the CMC. The data in Figure 7 imply a CMC of 0.006 M for **6**, although the fact that the data point nearest the intersection falls off the lines indicates that the aggregation process is not completely critical. Interestingly, this CMC is nearly identical to that of **7**, which contains a betaine headgroup and an 11-carbon linear tail.[21]

Self-Association in the Solid State. Crystal structures were determined for acids **1b**, **2b**, **4b**, and **5b**; Figures 8−11 show selected neighboring pairs (the crystal structure of **3b** has previously been reported[22]). The naphthyl groups in the crystal

(39) Shinoda, K.; Hutchinson, E. *J. Phys. Chem.* **1962**, *66*, 577.
(40) Ernst, R.; Miller, E. J. In *Amphoteric Surfactants*; Bluestein, B. R., Hilton, C. L., Eds.; Marcel Dekker, Inc.: New York, 1982; p 117.

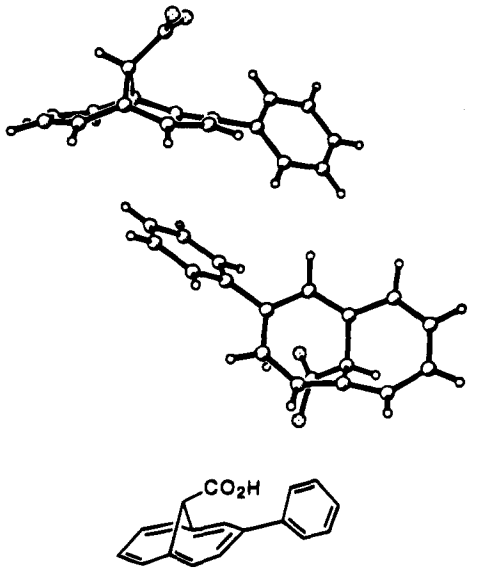

Figure 10. Ball-and-stick representation of a neighboring pair of molecules in the crystal lattice of **4b**. The closest approach involves the phenyl ring of the lower molecule and the annulene of the upper molecule; the angle between the mean planes of these two rings is 31°.

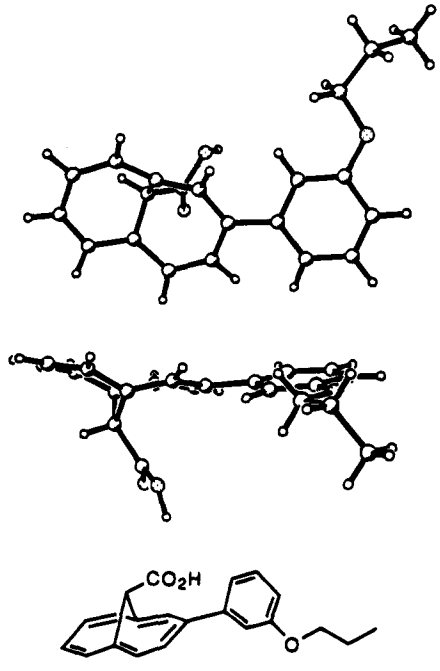

Figure 11. Ball-and-stick representation of a neighboring pair of molecules in the crystal lattice of **5b**. The annulene and phenyl rings of each molecule about the same neighbor. The interplanar angle between the annulene rings is 49°, and the interplanar angle between the phenyl rings is 81°.

of **2b** (Figure 9) occur in a "herringbone" pattern, an arrangement that is commonly observed for aromatic hydrocarbons in the solid state.[23] In **2b**, the angle between the planes of the adjacent naphthyl groups related in herringbone fashion is 48°, while in crystalline naphthalene the analogous angle is 51°.[24] The herringbone angle in **3b** is 86°.[25] A herringbone juxtaposition of neighbors is also observed for **1b** (Figure 8); in this case the angle between the mean planes of the annulene rings

(22) Rajan, S. S. *Acta Crystallogr.* **1978**, *B34*, 998.
(23) Desiraju, G. R.; Gavezzotti, A. *Acta Crystallogr.* **1989**, *B45*, 473.
(24) (a) Abrahams, S. C.; Monteath Robertson, J.; White, J. B. *Acta Crystallogr.* **1949**, *2*, 238. (b) Brock, C. P.; Dunitz, J. D. *Acta Crystallogr.* **1982**, *B38*, 2218 and references therein.

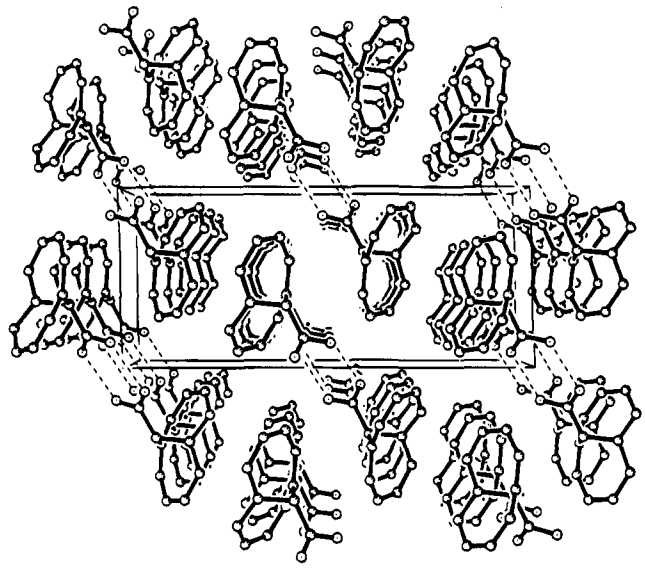

Figure 12. Packing pattern for **1b**. The hydrogen bonds between carboxylic acid groups are indicated by dashed lines.

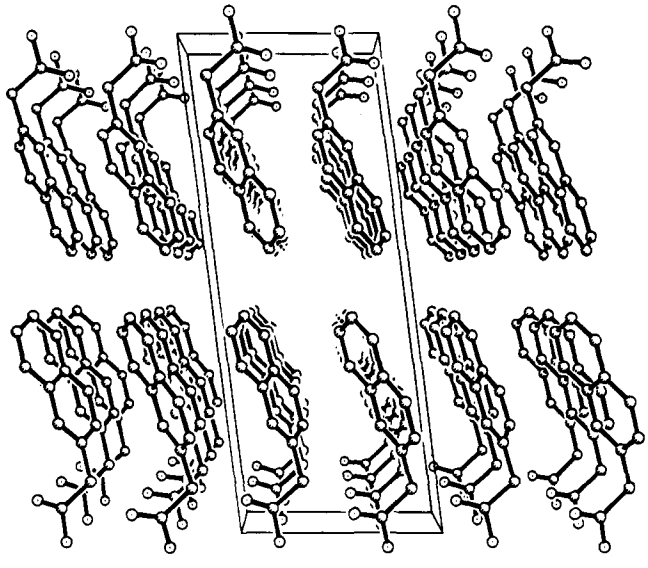

Figure 13. Packing pattern for **2b**. (The hydrogen bonded pairs are not shown.)

is 67°. In the crystal of **4b**, the closest approach to the "underside" of the annulene ring involves the phenyl ring of a neighboring molecule (Figure 10). The angle between the mean planes of these two aromatic groups is 31°. There is also a close phenyl–phenyl contact in crystalline **4b** (not shown), with a 34° angle between the two phenyl ring planes. The pattern of aromatic–aromatic interactions in the crystal of **5b** is quite different from that observed in **4b**. In **5b** (Figure 11), the phenyl rings are most closely associated only with other phenyl rings, and the annulene rings are most closely associated only with other annulene rings. The angle between the mean planes of the neighboring annulene rings is 49°, and the angle between the adjacent phenyl rings is 81°.

The crystal packing patterns for **1b**–**5b** are shown in Figures 12–16.[25] These packing patterns display a common structural theme: each crystal has a bilayer organization, with adjacent sheets of molecules connected to one another via carboxylic acid hydrogen bonds on one side and aromatic–aromatic

(25) The packing pattern shown for **3b** in Figure 14 was generated with data retrieved from the Cambridge Structure Data base: Allen, F. H.; Kennard, O.; Taylor, R. *Acc. Chem. Res.* **1983**, *16*, 46.

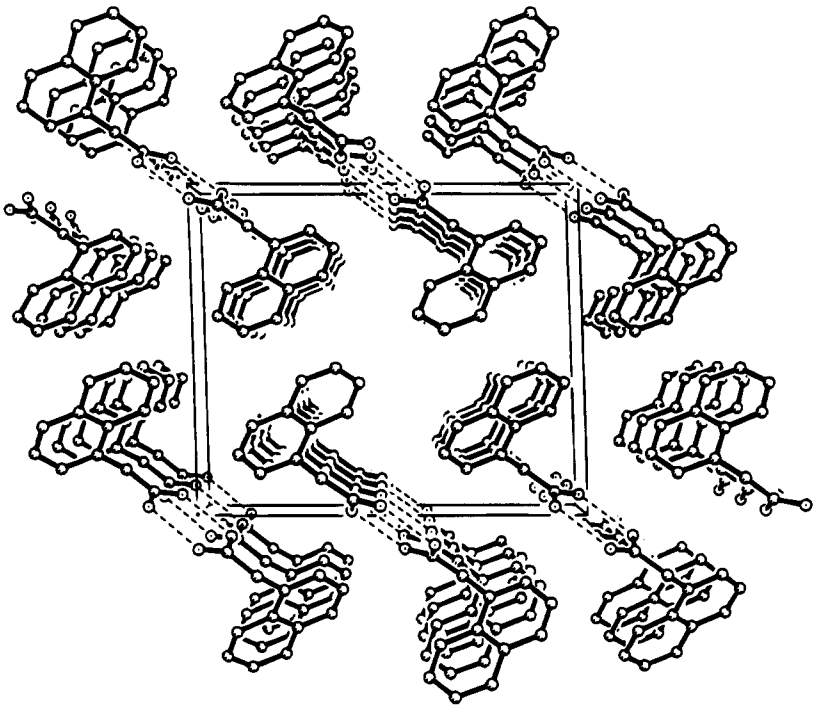

Figure 14. Packing pattern for **3b** (ref 25). The hydrogen bonds between carboxylic acid groups are indicated by dashed lines.

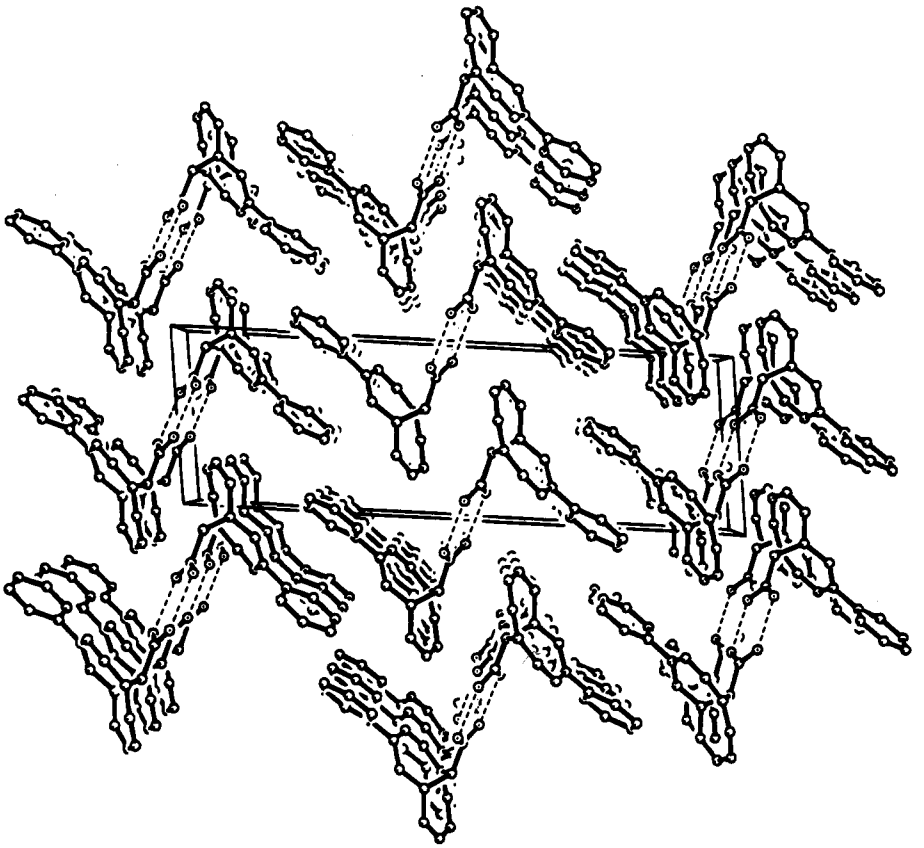

Figure 15. Packing pattern for **4b**. The hydrogen bonds between carboxylic acid groups are indicated by dashed lines.

contacts on the other side. The interlayer aromatic−aromatic contacts in **1b**, **4b**, and **5b** (Figures 12, 15, and 16, respectively) involve the herringbone juxtapositions illustrated by the neighboring pairs shown in Figures 8, 10, and 11. In contrast, the interlayer aromatic−aromatic contacts in **2b** (Figure 13) are "edge-to-edge"; the herringbone juxtapositions illustrated in Figure 9 correspond to interlayer contacts. For **3b** (Figure 14),[25] the interlayer contacts involve a herringbone arrangement.

Discussion

Solution Behavior. Comparison of contrafacial amphiphile **1a** to isomers of more conventional topology, **2a** and **3a**, via tensiometry and dye solubilization provides support for the contrafacial amphiphile hypothesis. These studies suggest that naphthylacetates **2a** and **3a** can arrange themselves in two- or

(26) Bryson, A. *J. Am. Chem. Soc.* **1960**, *82*, 4862.

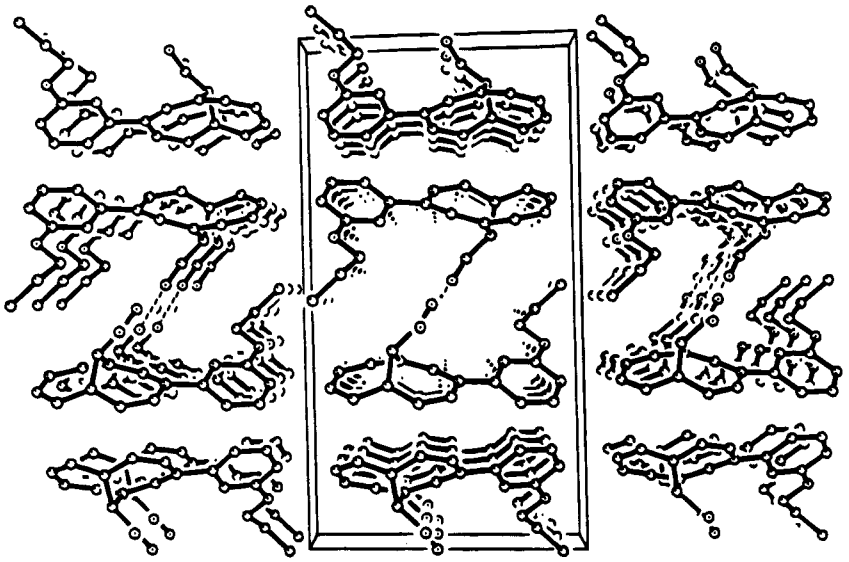

Figure 16. Packing pattern for **5b**. The hydrogen bonds between carboxylic acid groups are indicated by dashed lines.

three-dimensional arrays (at the air–water interface or in bulk solution, respectively) that minimize hydration of the nonpolar naphthyl moieties. In contrast, the minimal effect of **1a** on surface tension and the inability of **1a** to solubilize orange OT suggest that this molecule's distinctive amphiphilic topology precludes effective self-association of nonpolar surfaces in two- or three-dimensional arrays. Rigid extention of the contrafacial amphiphile's nonpolar surface does not lead to enhanced self-association, as indicated by the lack of orange OT solubilization by **4a**. A short, flexible additional nonpolar extention to form **5a**, however, leads to more avid aggregation, according to dye solubilization results and the concentration-dependence of the ^{1}H NMR chemical shifts of **5a**.

Because the NMR and dye solubilization data for 1,6-methano[10]annulene-based amphiphiles **1a**, **4a**, and **5a** suggest that these molecules self-associate relatively weakly in aqueous solution (and perhaps not at all for **1a** and **4a**), it was important to determine whether the bridged annulene skeleton is intrinsically antithetical to cooperative self-association. The behavior of **6** demonstrates that a relatively small amphiphile containing this structural unit can indeed undergo cooperative aggregation (presumably micelle formation). This result may be compared to our previous findings with amphiphiles **8**, **9**, and **10a–g**, all

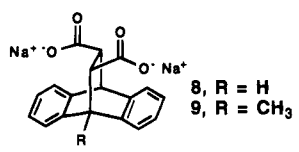

8, R = H
9, R = CH_3

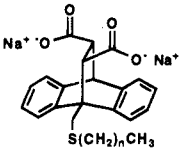

10a, n = 0
10b, n = 1
10c, n = 3
10d, n = 5
10e, n = 7
10f, n = 9
10g, n = 11

based on an ethanoanthracenedicarboxylate contrafacial amphiphile unit.[15] Self-association of the smaller members of this family, **8**, **9**, and **10a,b**, is non-cooperative, but aggregation becomes increasingly cooperative as the flexible nonpolar "tail" is lengthened. Amphiphile **10g** behaves like a typical micelle-forming detergent, with a CMC of 0.003 M, as measured by both NMR and dye solubilization techniques.[13]

Comparison of the CMC values for **10c–g** with analogous 2-alkylated malonate surfactants allowed us to conclude that the "hydrophobic impact" of the 16-carbon ethanoanthracene unit, when placed at the polar end of a flexible amphiphile, is equivalent to only five CH_2 units in an alkyl tail.[13] This equivalency is surprisingly small, since similar comparisons have indicated that a phenyl group in a flexible alkyl tail is equivalent to approximately three and one-half CH_2 units.[1a] We cannot come to any firm quantitative conclusions about the hydrophobic impact of the bridged annulene unit, because we have not examined a homologous series related to **6**. Nevertheless, the similarity of the CMC values for **6** and the more conventional amphiphile **7** suggests that the 17-carbon 3-phenyl-1,6-methano-[10]annulene unit promotes self-association to the extent of no more than six CH_2 units in a long alkyl chain (the presence of two internal polar elements in **6**, the amide group and the ether oxygen, allows only a very approximate comparison to **7**).

Solid State Data. The observed carboxylic acid crystal packing patterns allow one to generate specific explanations for the low surface activity of contrafacial amphiphile **1a** relative to those of more conventional isomers **2a** and **3a**. Rationalizing the interfacial behavior of these carboxylates on the basis of crystal packing data for the conjugate acids requires many assumptions, and any extrapolation from the solid state to solution must be regarded as tentative. Nevertheless, it is reasonable to use patterns observed among crystal data to formulate working hypotheses regarding the behavior of amphiphiles **1a–3a** at the air–water interface.

The individual layers observed in the crystals of **2b** and **3b** (Figures 13 and 14) serve as models for monolayers of **2a** and **3a** at the air–water interface. These crystallographically observed layers suggest that each of the naphthylacetates can form a two-dimensional array in which all polar groups are oriented in a common direction (i.e., into the aqueous phase), and all hydrocarbon fragments extend into the gas phase. The layer structure observed for acid **1b**, on the other hand, suggests that parallel orientation of polar groups within an amphiphilic layer of **1a** would require that a substantial fraction of the hydrocarbon skeleton be in contact with an adjacent polar layer (e.g., the aqueous phase).

Conclusions. We have shown that the topological relationship between the polar and nonpolar surfaces of an amphiphile exerts a substantial effect on behavior in aqueous solution. Conventional amphiphiles **2a** and **3a** have a significant tendency to partition to the air–water interface, but contrafacial amphiphile **1a** does not. In bulk aqueous solution, contrafacial amphiphile **1a** aggregates less avidly than isomers **2a** or **3a** (indeed, **1a** may not aggregate at all). Hydrophobic dye solubilization is impossible for **1a**, and remains impossible when the nonpolar contrafacial amphiphile skeleton rigidly extended, to form **4a**; however, appending a relatively short flexible

nonpolar segment to the contrafacial amphiphile skeleton (to form **5a**) leads to effective dye solubilization. These distinctive properties of contrafacial amphiphiles suggest that they may display unique behavior toward biological membranes, a prospect that is currently under examination in our laboratory.

Experimental Section

Synthesis of Amphiphile 6. Compound **4b** (254 mg, 0.79 mmol) was dissolved in 150 mL of distilled benzene containing 20 μL of distilled DMF under N_2. After this solution had been cooled with an ice bath to near its freezing point, oxalyl chloride (690 μL, 7.9 mmol) was added dropwise, leading to the evolution of a gas. The yellow solution was stirred for 5.5 h, and then all volatiles were removed *in vacuo*. A N_2 atmosphere was reestablished, the oily residue was taken up in 100 mL of dry Et_2O, and *N,N*-dimethylethylenediamine (104 μL, 0.95 mmol) was added, causing precipation of a white solid. The mixture was stirred for 18 h and then washed with 35 mL of 1 N NaOH and dried over $MgSO_4$. Removal of solvent left a tan oil that was purified by column chromatography on silica, eluting with 5% NH_3-saturated CH_3OH in CH_2Cl_2, to afford the desired (dimethylamino)-ethylamide of **4b** as a yellow oil (244 mg, 79%): ^{1}H NMR (200 MHz, $CDCl_3$) δ 0.74 (s, 1H), 1.05 (t, J = 7.35 Hz, 3H), 1.82 (m, 2H), 2.08 (s, 6H), 2.11 (t, J = 6 Hz, 2H), 2.89 (m, 2H), 3.96 (t, J = 6.6 Hz, 2H), 5.58 (t, J = 4.7 Hz, 1H), 6.84−6.90 (m, 1H), 7.00−7.04 (m, 2H), 7.14−7.18 (m 2H), 7.26−7.34 (m, 2H), 7.47−7.60 (m, 4H); ^{13}C NMR (67.5 MHz, $CDCl_3$) δ 10.49, 22.56, 36.24, 44.98, 50.12, 57.46, 69.46, 112.78, 115.08, 115.85, 116.23, 120.43, 125.93, 126.13, 126.25, 128.33, 129.34, 130.25, 130.78, 139.44, 145.22, 159.21, 166.28; IR (film) 3500−3300 (br), 2964, 2938, 2875, 1664, 1604, 1596, 1576, 1508, 1489, 1288, 1192, 778 cm^{-1}; high res. EI MS *m/z* 390.2344 (calcd for $C_{25}H_{30}N_2O_2$ 390.2341).

A mixture of this amino amide (118 mg, 0.30 mmol), 5.33 mL of 68 mM aqueous NaOH (0.36 mmol), and α-bromoacetic acid (50 mg mmol) was heated to reflux for 60 h. At this point, more α-bromoacetic acid (12 mg, 0.09 mmol) and base (1.32 mL of 68 mM NaOH, 0.09 mmol) were added, and the mixture was refluxed for an additional 31 h. (Reaction progress was monitored via C_{18} reverse phase silica TLC, eluting with 0.1 M NH_4OAc in 4:1 CH_2OH:H_2O that had been adjusted to pH 6.8 by addition of acetic acid (solvent system B).) After cooling, the brown reaction solution was applied to a C_{18} reverse phase phase silica column pre-equilibrated with 0.05 M aqueous NH_4OAc that had been adjusted to pH 6.8 with NH_4OH (solvent system A). Elution with this solvent removed inorganic salts, as indicated by a $AgNO_3$ halide test. The column was then eluted with mixtures of solvent systems A and B containing increasing proportions of B, and finally with CH_3OH. Fractions containing the desired product were pooled, and CH_3OH was removed via rotary evaporation. Water and NH_4OAc were then removed by lyophilization, affording a pale yellow solid (90 mg, 67%): mp 115−117 °C (dec); ^{1}H NMR (270 MHz, D_2O; 2 mM) δ 0.92 (s, 1H), 1.02 (t, 3H, J = 7.6 Hz), 1.81 (m, 2H), 2.97 (s, 6H), 3.23 (br s, 4H), 3.62 (s, 2H), 4.11 (t, 2H, J = 6.6 Hz), 7.03−7.48 (m, 7H), 7.63 (br s, 4H); ^{13}C NMR (67.5 MHz, CD_3OD) δ 10.94, 23.74, 34.17, 51.43, 51.87, 63.18, 65.16, 70.62, 114.22, 115.91, 116.74, 117.38, 121.78, 126.83, 127.16, 127.29, 127.50, 129.47, 130.83, 131.31, 132.03, 140.27, 146.39, 160.88, 168.31, 169.85; IR (CH_2Cl_2) 3700−2800 (br), 2967, 1643, 1607, 1527, 1477, 1392 cm^{-1}; low res. FAB MS *m/z* 449 (calcd for $C_{27}H_{33}N_2O_4$ (M + H) 449).

Sodium carboxylates 1a−5a were prepared from the corresponding carboxylic acids, **1b−5b**, by mixture with 2−5% molar excess of standardized aqueous NaOH (semiconductor grade NaOH from Aldrich Chemical Co. was used). The resulting clear solutions were lyophilized and then further dried over P_2O_5 under vacuum at room temperature for 2 days. When these salts were dissolved in deionized (Millipore) water, the solutions were always mildly basic. For example, a 0.35 M solution of **1a** had a pH of 9.6, a 0.003 M solution of **1a** had a pH of 7.6, a 0.35 M solution of **2a** had a pH of 10.7, and a 0.003 M solution of **2a** had a pH of 9.6. We determined the pK_a of **1b** to be 4.2, which is nearly identical to the reported pK_a values of **2b** and **3b**.[26]

Surface Tension Studies. Carboxylic acids **1b−3b** were recrystallized until each gave a constant melting point. These acids were dried overnight under vacuum in the presence of P_2O_5 and then dissolved in a solution of pretitrated semiconductor grade NaOH, containing a small molar excess of base. The resulting solutions were lyophilized, and the sodium carboxylate salts were dried 24 h under vacuum in the presence of P_2O_5. Prior to the surface tension measurements, a stock solution of each salt was prepared and passed through a 0.22 μm filter. Surface tension measurements were performed with a Federal Pacific Electric Co. Model LG tensiometer fitted with a Wilhelmy plate. When concentrations were changed, the surface was allowed to equilibrate for 3−5 min; the plate was submerged during this time. Amphiphile concentrations were varied via serial dilution or serial concentration, both methods giving the same results. Each measurement was performed in quadruplicate, and each experiment was performed in triplicate.

Aggregation Studies via Dye Solubilization. Orange OT was purified by water precipitation from an acetone solution, followed by two recrystallizations from EtOH.[21] Amphiphile solutions in D_2O were prepared as described in the preceding paragraph and transferred to screw-capped vials, and excess solid orange OT was added. The mixtures were agitated gently at room temperature for 2−3 days with a blood-rocker. The mixtures were then filtered through cotton to remove undissolved orange OT, and 200 μL aliquots of the filtrate were diluted with 800 μL of absolute EtOH. The absorbance of each solution at 500 nm was measured with a 1 cm path length cell. Based on the UV data, the following dye:amphiphile ratios were deduced: 0.6 M **2a**, 1:5000; 0.6 M **3a** 1:16000; 0.08 M **5a**, 1:7700.

Aggregation Studies via ^{1}H NMR. A 2 or 5 mL stock solution near the saturation point was prepared by dissolving a weighed amount of each solid amphiphile in low-conductivity D_2O from MSD Isotopes. Samples for spectroscopic characterization were obtained by dilution. Spectra were obtained on a Bruker WP-270 spectrometer using external TSP as reference.

Crystal Growth. X-ray quality crystals of **1b**, **4b**, and **5b** were obtained by dissolving these compounds in a minimum amount of hot EtOAc, allowing the resulting solution to cool, and then allowing the solvent to evaporate slowly. For **4b**, this procedure provided crystals with two morphologies, needles and clusters of prisms; the crystal structure was obtained from the needles. 2-Naphthylacetic acid (**2b**) was dissolved in CH_2Cl_2, and the solvent was allowed to evaporate slowly, providing large thin plates.

Acknowledgment. This research was supported by the National Institutes of Health (GM-41825). We thank the reviewers for helpful suggestions and Ms. Jane Klassen and Prof. Gil Nathanson for assistance with the surface tension measurements. J.M.D. was supported in part by the Graduate Assistance in Areas of National Need Program. S.H.G. is a Fellow of the Alfred P. Sloan Foundation.

JA942434Y